Construction and Building Materials 292 (2021) 123389

Contents lists available at ScienceDirect

Construction and Building Materials

journal homepage: www.elsevier.com/locate/conbuildmat

Continuous monitoring of early-age properties of sprayed mortars by *in situ* ultrasound measurements

F. Pellegrino [a], R. Salvador [b], S. Aparicio [d], M.G. Hernández [d], J.J. Anaya [d], S.H.P. Cavalaro [e], I. Segura [a,c,*]

[a] Department of Civil and Environmental Engineering, Universitat Politècnica de Catalunya - Barcelona Tech, C/Jordi Girona 1-3, C1, 08034 Barcelona, Spain
[b] Department of Civil Engineering, São Judas Tadeu University, 546 Taquari St, 03166-000 São Paulo, Brazil
[c] Smart Engineering Ltd, C/Jordi Girona 1-3, Parc UPC – K2M, 08034 Barcelona, Spain
[d] Institute of Physical and Information Technologies Leonardo Torres Quevedo (ITEFI), CSIC, C/Serrano 114, 28006 Madrid, Spain
[e] School of Architecture, Building and Civil Engineering, Loughborough University, Leicestershire LE11 3TU, UK

HIGHLIGHTS

- Sprayed mortars were analyzed with a novel *in situ* ultrasonic continuous monitoring system.
- Continuous monitoring of early age properties was possible without drawbacks.
- The system can also characterize the reactivity between cement and accelerator.
- 4 hydration stages were delimited in the ultrasonic curves as in calorimetry.
- Correlations are provided between ultrasound and penetration resistance.

ARTICLE INFO

Article history:
Received 16 November 2020
Received in revised form 23 February 2021
Accepted 13 April 2021
Available online 21 May 2021

Keywords:
Sprayed mortar
Hydration
Early age properties
Ultrasound measurements

ABSTRACT

The development of early age properties of sprayed concrete is a key factor that governs its mix design and safe application. The conventional methods to evaluate the evolution of mechanical strength in sprayed concrete present a large interval between each set of measurements and results present a high scatter. In this context, the objective of this study is to characterize the early age properties of sprayed mortars through a novel continuous monitoring system based on *in situ* ultrasound measurements. Sprayed mortars were also analyzed by isothermal calorimetry, needle penetration and stud driving method. Results indicate that the system developed here can monitor the evolution of early age properties of sprayed mortars continuously without the common drawbacks observed in penetration tests. This research may lead to the development of a more reliable procedure to characterize the early age mechanical properties of sprayed materials in the worksite under safer conditions.

1. Introduction

Sprayed concrete is a construction process applied widely for the stabilization of slopes and tunnel excavation fronts [1,2]. The evolution of early age properties of sprayed concrete is the key parameter that governs its mix design, applicability and proper placement. The technological control of the spraying process is fundamental to ensure the required structural support to the unstable ground and to prevent dangerous fallouts of large masses of fresh material from walls and overhead areas [3].

The characterization of the mechanical strength of sprayed concrete at early ages is usually performed by needle penetration [4,5] and by the stud driving method [6], following the recommendations of UNE EN 14488-2 [7]. These tests are discontinuous in time, that is, present a large interval between each set of measurements. In addition, results present a high scatter (from 10 to 30%, approximately [8]) and depend significantly on the experience and ability of the operator. Furthermore, the *in situ* execution of these tests entails exposing workers to unsafe conditions.

Over the last decades, promising outcomes have been reported on the application of ultrasound (US) techniques to monitor the development of microstructure and mechanical properties of cementitious matrices [9–13]. A great effort has been made to find correlations between the evolution of early age properties of concrete and ultrasonic parameters, such as wave transmission

* Corresponding author at: Department of Civil and Environmental Engineering Universidad Politécnica de Cataluña - BarcelonaTech Campus Nord - Eficio B1 - Despacho 104B Calle Jordi Girona Salgado, 1-3 08034, Barcelona, Spain.
E-mail address: ignacio.segura@upc.edu (I. Segura).

https://doi.org/10.1016/j.conbuildmat.2021.123389
0950-0618/

[14–17], wave reflection [11,18,19] and wave attenuation [20,21]. These methods provide a relatively simple approach to assess the strength evolution of concrete during construction.

Despite the substantial work conducted on the characterization of conventional concrete, a reduced number of studies addressed the application of ultrasound techniques in sprayed concrete technology. De Belie et al. [22] and Salvador et al. [23] presented meaningful results on the characterization of the reactivity of accelerators for sprayed concrete by ultrasound monitoring, confirming the potential application of the technique to evaluate the early age properties of the fast hydrating matrix. Nevertheless, these studies were performed with mechanically mixed mortars containing accelerators. Therefore, it is necessary to characterize sprayed materials by ultrasound measurements, to provide a deeper knowledge of the relationship between the evolution of early-age mechanical properties and ultrasound velocity.

In this context, the objective of this study is to evaluate the early age properties of sprayed mortars through a novel continuous monitoring system based on *in situ* ultrasound measurements conducted in laboratory-controlled conditions. The instrumented panel developed could monitor the evolution of early age properties of sprayed mortars continuously, overcoming several limitations found in the execution of penetration tests. Significant changes were observed in the behavior of sprayed mortars depending on the type and dosage of the accelerator employed, indicating the system could characterize the reactivity between cement and accelerator. This method may result in a potential system to characterize sprayed materials continuously in field applications. In addition, it requires no operator, which may contribute to reduce the number of workers exposed to risky conditions during tunnel construction.

2. Experimental methodology

2.1. Materials

All experiments were conducted with mortars produced with CEM I 52.5R, containing 4.7% of C_3A, a C_3A/SO_3 molar ratio equal to 0.39 and a specific weight equal to 3.10 g/cm^3. The XRD, FRX and physical characterization of this cement may be found in a previous research [13]. Based on the XRD mineralogical composition of the cement, its total heat of hydration was equal to 433 J/g, considering the relative sum of the heats of hydration of the individual phases (C_3S: 510 J/g; C_2S: 260 J/g; C_3A: 1100 J/g; C_4AF: 410 J/g [24]).

A calcareous sand ($CaCO_3$ > 90%, specific weight = 2.42 g/cm^3, water absorption = 5.5% by mass) was used. The sand particle size distribution ranged from 0 to 1 mm, which was a requirement for the correct operation of the pumping and spraying system. Distilled water and a superplasticizer based on a polycarboxylate ether solution (solid content = 34%, specific weight = 1.09 g/cm^3) were used.

Two alkali-free accelerators composed by aluminum sulfate solutions were selected to cover the types commonly found in practice. They contain different aluminum/sulfate ratios and their nomenclature corresponds to '*AF Al_2O_3/SO_4^{2-} molar ratio*'. In addition, an alkaline accelerator based on sodium aluminate, identified as '*AK*', was also employed. The composition and properties of accelerators are summarized in Table 1.

2.2. Composition of mortars

All mortars had a water/cement ratio equal to 0.51 and an aggregate/cement ratio equal to 1.7. Superplasticizer dosage was 1.0% by cement weight (% bcw). The resulting fresh mortar presented air content equal to 2.1% by volume, specific weight equal to 2.05 g/cm^3, spread diameter equal to 300 mm and no bleeding. Although the elevated cement content in the mix design (638 kg/m^3), this mortar composition was required to comply with the workability and pumpability required for the proper operation of the spraying equipment. It is important to mention that the mortar was designed only for laboratory tests, aiming at the characterization of the chemical behavior of accelerators and its influence on the monitoring of the hardened mortar by ultrasound measurements. It was not intended to employ this mix design for structural applications.

Table 1
Composition and properties of accelerators.

Property	AF 0.59	AF 0.61	AK
Dry matter content (%)	40.0	34.5	43.0
Al_2O_3 content (%)	12.5	13.5	24.0
SO_4^{2-} content (%)	20.0	21.0	Not applicable
Na_2O content (%)	Not applicable	Not applicable	19.0
Al_2O_3/SO_4^{2-} molar ratio	0.59	0.61	Not applicable
Stabilizing agent	Organic acid	Inorganic acid	Not applicable
pH at 20 °C	3.2	3.0	12.0
Specific weight (g/cm^3)	1.37	1.47	1.52

Accelerator AF 0.59 was used at 3.5, 5.0, 8.0 and 10.0% bcw, AF 0.61 was added at 5.0, 8.0 and 10.0% bcw and AK was used at 3.0, 5.0 and 10.0% bcw. These dosages were determined according to [8] to guarantee equivalent setting development in cement pastes and fall within limits usually employed sprayed concrete applied in tunnel linings. Mortars were identified by '*accelerator name_accelerator dosage*'.

Table 2 presents the final C_3A/SO_3 ratio of each mortar, determined according to Salvador et al. [25]. This parameter indicates if the mortar is properly or under-sulfated after accelerator addition and may be used to predict if accelerated C_3A reactions occur during early hydration. The sulfate balance of the mortar will be used for further discussion of results.

2.3. Preparation of mortars

Batches containing 60 L of mortar were produced for each spraying session, using a planetary mortar mixer type 65/2 K-3, with paddle rotation and planetary speed equal to 150 and 40 rpm, respectively. Cement and 90% of the total amount of water were mixed for 240 s. After that, the internal wall of the container was scraped. Then, the remaining amount of water and the superplasticizer were added and mixed for 240 s. Finally, fine aggregate was added and homogenized for 300 s. Accelerators were incorporated in the spraying process 1 h after cement and water had been mixed, following previous experiences from the research group [13,25].

2.4. Spraying process

A laboratory-scale mortar spraying equipment, whose detailed description may be found in a previous paper from the research group [25], was employed. This equipment consists of a helical screw pump coupled with a 3-HP air compressor, a flowmeter to dose accelerators and a spraying gun and a nozzle developed specifically for this study. The spraying gun contained three different inlets for the ingress of fresh mortar, compressed air and liquid accelerators. The nozzle had a frustum shape (base diameter = 14.0 mm, top diameter = 8.0 mm, height = 10.0 mm, presenting 6 holes at its base for the inlet of accelerator and compressed air).

The whole spraying process was performed in a thermally insulated climatic chamber kept at 20 °C and 50% relative humidity.

Table 2
Final C_3A/SO_3 ratio of mortars.

Phase/compound	AF 0.59_3.5%	AF 0.59_5.0%	AF 0.59_8.0%	AF 0.59_10%	AF 0.61_5.0%	AF 0.61_8.0%	AF 0.61_10%	AK_3.0%	AK_5.0%	AK_10%
Total sulfate in cement (mmol/g cement)	0.441	0.441	0.441	0.441	0.441	0.441	0.441	0.441	0.441	0.441
Aluminum in ccelerator (mmol/g cement)	0.086	0.123	0.196	0.245	0.132	0.212	0.265	0.141	0.235	0.471
Sulfate in accelerator (mmol/g cement)	0.146	0.208	0.333	0.416	0.219	0.350	0.437	0.000	0.000	0.000
Ettringite formed by accelerator reaction (mmol/g cement)	0.043	0.061	0.098	0.123	0.066	0.106	0.132	0.071	0.118	0.147
AFm phases formed by accelerator reaction (mmol/g cement)	–	–	–	–	–	–	–	–	–	0.227
Sulfate consumed in ettringite formation (mmol/g cement)	0.129	0.184	0.294	0.368	0.199	0.318	0.397	0.212	0.353	0.441
Sulfate left after accelerator reaction (mmol/g cement)	0.458	0.465	0.480	0.490	0.461	0.473	0.481	0.229	0.088	0.0
Final C_3A/SO_3 molar ratio	0.38	0.37	0.36	0.36	0.38	0.37	0.36	0.76	1.98	Not applicable

Mortars were sprayed into trapezoidal metallic panels designed according to EN 14488–1 [26] (base = 300 mm × 300 mm, top = 450 mm × 450 mm, height = 70 mm) and into prismatic wood panels (length = 400 mm, width = 200 mm, height = 70 mm). Metallic panels were used to perform pin penetration tests and to assess the ultrasound propagation velocity of the mortars, while wood panels were employed to conduct needle penetration tests.

All the panels were kept inside the chamber during spraying. The distance from the exit of spraying gun to the panels was 1.0 m and the gun was positioned to conduct spraying perpendicularly to the bottom of the panels. The optimal fresh mortar flow was set to 5.0 L/min and the accelerator flow was determined according to accelerator type and dosage.

2.5. Test methods

Sprayed mortars were characterized by the tests summarized in Table 3. All the tests are described subsequently and were performed considering accelerator addition as the start (time 0).

2.5.1. Isothermal calorimetry

Isothermal calorimetry was conducted to analyze the influence of accelerators on cement hydration kinetics in sprayed mortars. Tests were performed at 20 °C during 24 h with 35 g of sprayed mortar, using an I-cal 4000 isothermal calorimeter. Mortars were sprayed directly in the cups and placed in the equipment immediately after spraying.

2.5.1.1. Needle penetration test. Needle penetration test was performed to determine the penetration resistance of sprayed mortars. It is equivalent to the penetrometer test prescribed by UNE EN 14488-2 [7], employed to determine the compressive strength of sprayed concrete up to 1 MPa and to classify the evolution of mechanical strength as either J_1, J_2 or J_3. The test performed was an adaptation of the procedure from ASTM C-403 [4] to provide a constant rate of needle penetration. Therefore, the test was conducted in a displacement-controlled testing machine, as shown in Fig. 1, at a constant penetration rate equal to 60 mm/min.

Cylindrical needles with diameters equal to 20.3, 14.3, 9.0, 6.4 and 4.5 mm were selected to obtain the minimum force of 100 N when the penetration reached 25 mm. The penetration resistance was obtained by dividing the penetration load by the sectional area of the needle. This test was conducted from 15 min until the penetration resistance reached 27.6 MPa, since this value corresponds to the final setting defined in ASTM C-403 [4]. An average of five penetrations was calculated at each age.

2.5.1.2. Pin penetration test. Pin penetration test (Fig. 2.a) was performed to determine the indirect compressive strength of sprayed mortars. It is equivalent to the stud driving method prescribed by UNE EN 14488–2 [7], employed to determine the compressive strength of sprayed concrete from 2 MPa on. The results obtained by this test are also employed to classify the evolution of mechanical strength as either J_1, J_2 or J_3.

A Windsor WP-2000® pin system (Fig. 2.b) was used for this test, instead of the commonly used Hilti® gun [7] due to the limitation of the panels sizes. The pin penetration depth was determined using a micrometer and the compressive strength was calculated based on a correlation table given in the technical manual of the equipment [29]. An average of five penetrations was calculated at the ages of at 4, 6, 8, 10, 12 and 24 h after spraying.

2.5.1.3. In situ ultrasound measurements. An ultrasound monitoring system was used to monitor the evolution of early-age properties of sprayed mortars continuously. This system is named

Table 3
Tests performed with accelerated pastes and mortars.

Test	Specimen	Age/period	Reference
Isothermal calorimetry	Mortar in fresh state	0–24 h	[27]
Needle penetration test	Mortar in wood panels	From 15 min to final setting	[4]
Pin penetration test	Mortar in metal panels	4, 6, 8, 10, 12 and 24 h	[7]
Determination of ultrasound propagation velocity	Mortar in metal panels	0–24 h	[28]

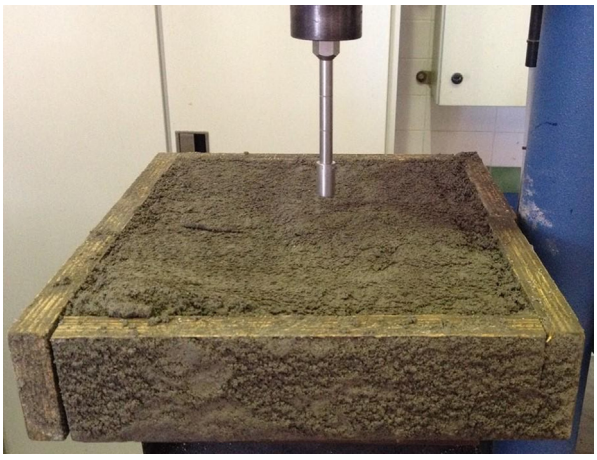

Fig. 1. Penetration resistance test.

(a)

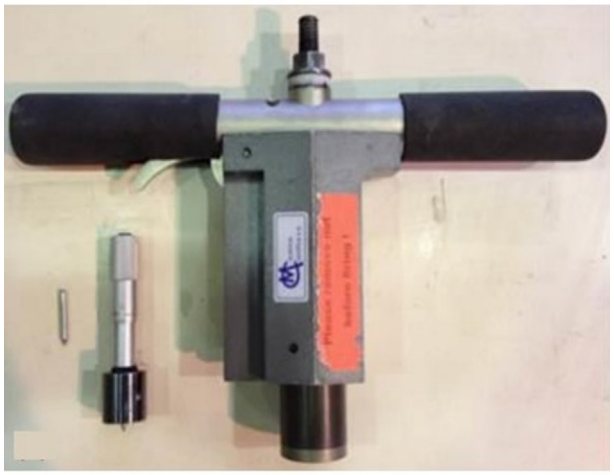

(b)

Fig. 2. Execution of the pin penetration test (a) and the Windsor WP-2000® pin system used (b).

WilTempUS-II and was developed by ITEFI Institute from the Spanish National Research Council [30,31]. It contains two wireless sensor networks coupled with 54 kHz ultrasound transducers, which generate and receive longitudinal ultrasonic signals.

The detailed description of the instrumented panes used in this study is presented in a previous paper published by the research group [28]. It contains 2 transducers, which were embedded in metal cones and installed on a spraying panel, 200 mm distant from each other (Fig. 3). The cones improve the contact of the transducer with the mortar thereby enhancing ultrasound transmission [28]. The panels were separated from the floor by rubber bearings to reduce the noise that could affect the quality of the measurements. The ultrasound propagation velocity was determined every 5 min, from the time of spraying until 24 h. The signal was processed in a python application designed specifically for the system [28].

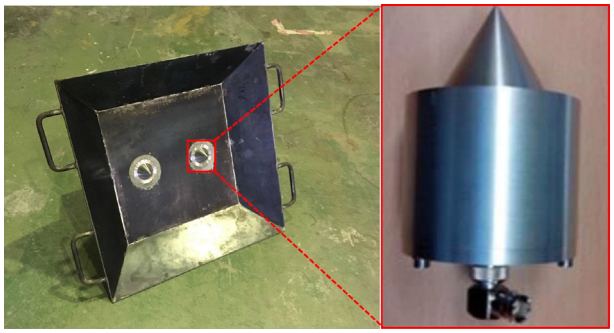

Fig. 3. Spraying panel instrumented with 2 transducers embedded in metal cones.

3. Results and discussion

3.1. Isothermal calorimetry

The heat flow curves of sprayed mortars produced with accelerators AF 0.59, AF 0.61 and AK are presented in Fig. 4.a, 2.b and 2.c, respectively. Results are shown from 0 to 18 h to provide a detailed presentation of each curve. Table 4 summarizes the characteristic points of the heat flow curves, determined according to Salvador et al. [32]. Fig. 5 illustrates the degree of hydration of the sprayed mortars, considering the area under the heat flow curves from accelerator 0 to 24 h, divided by the total heat of hydration of the cement employed (433 J/g).

A fast and highly exothermic ettringite formation reaction occurs immediately after the addition of the accelerator [27,33]. This reaction consumes calcium and sulfate ions from the liquid phase, leading to the dissolution of gypsum and alite to balance the concentration of these ions. Therefore, induction periods are reduced when accelerators are employed, taking for comparison sprayed mortars produced with no accelerator in the studies of Salvador et al. [25] and Herrera et al. [13].

In general, induction periods are the shortest in mortars with AF 0.59, when compared to mortars containing AF 0.61 and AK with similar amounts of Al_2O_3 derived from the accelerator. As accelerator AF 0.59 provides the smallest amount of aluminum ions, the smallest amount of ettringite is formed by accelerator reaction (see Table 4). Therefore, the onset of the main hydration peak occurs earlier in mortars containing AF 0.59, because the amount of ettringite formed does not suppress alite hydration due to lack of space [32,34].

As alite hydration is the least inhibited by ettringite formation in mortars containing AF 0.59, the hydration rate and the maximum heat flow reached in the main hydration peak are the highest. Also, the energy released in the main hydration peak in these mortars is higher than in mortars produced with accelerators AF 0.61 and AK. The only exception is mortar AF 0.59_10%, where the large amount of aluminate hydrates formed by accelerator reaction fills up the space in the matrix and retard the onset of alite hydration as observed in [32,34].

In mortars produced with AF 0.61, the reaction rate, maximum heat flow and energy released in the main hydration peak are lower than in mortars containing AF 0.59. This was expected as AF 0.61 contains 8% more Al_2O_3 in its composition, which leads to a larger amount of ettringite and suppresses alite hydration due to lack of space. Furthermore, this accelerator contains an inorganic acid as a stabilizing agent. Since phosphoric acid is the main inorganic compound employed to that end, alite hydration may be suppressed due to the precipitation of calcium phosphate on the surface of cement particles, reducing their solubility and further hydration [35].

Cement hydration is significantly affected when accelerator AK is employed and mortars behave as under-sulfated. Since this accelerator does not contain sulfate in its formulation, sulfate depletion occurs fast, leading to mortars with high C_3A/SO_3 ratios (see Table 4). It may be observed that sulfate content in cement is not enough to lead to ettringite formation when AK is used at 10% and AFm phases may be formed by accelerator reaction.

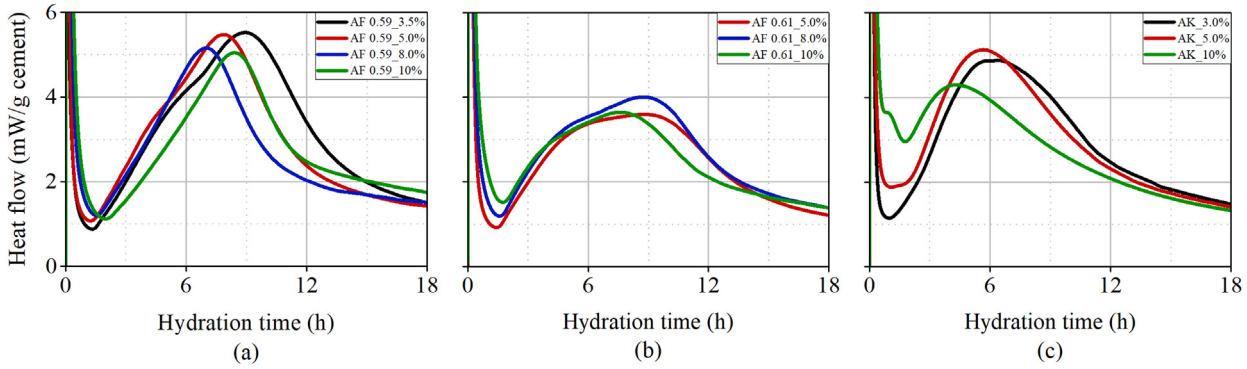

Fig. 4. Heat flow curves of sprayed mortars containing accelerator AF 0.59 (a), AF 0.61 (b) and AK (c).

Table 4
Parameters derived from heat flow curves of sprayed mortars.

Mortar	Induction period (h)	Slope acceleration - main peak (mW/g.h)	Maximum heat flow - main peak (mW/g)	Time to reach the maximum heat flow (h)	Energy released - main peak (J/g)
AF 0.59_3.5%	1.5	0.792	5.52	9.0	235.8
AF 0.59_5.0%	1.4	0.841	5.47	7.9	222.1
AF 0.59_8.0%	1.8	0.806	5.16	7.0	200.5
AF 0.59_10%	2.4	0.640	5.05	8.5	195.8
AF 0.61_5.0%	1.7	0.738	3.60	8.7	157.7
AF 0.61_8.0%	1.8	0.785	4.01	8.8	176.0
AF 0.61_10%	1.9	0.731	3.65	7.6	157.3
AK_3.0%	1.5	1.04	4.88	5.6	213.8
AK_5.0%	1.1	1.21	5.13	4.5	209.9
AK_10%	0.7	0.865	4.30	5.3	175.3

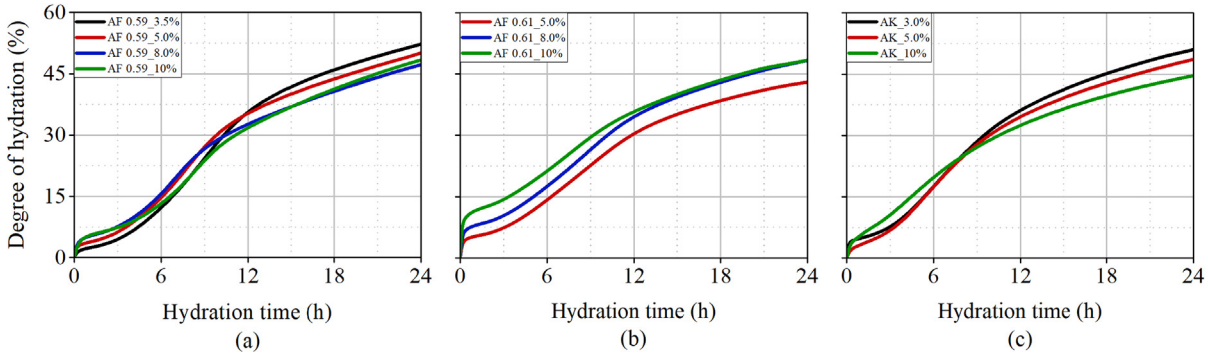

Fig. 5. Degree of hydration of sprayed mortars containing accelerator AF 0.59 (a), AF 0.61 (b) and AK (c).

Moreover, the fast sulfate depletion accelerates C_3A hydration. As observed in Fig. 4.c, the main hydration peak does not present the shoulder related to secondary ettringite formation after the ascending part of the curve, as observed when accelerators AF 0.59 and 0.61 are employed. C_3A and alite hydration occur concomitantly, leading to faster reaction rates and higher values of maximum heat flow in the main hydration peak. As C_3A hydration is accelerated, the degree of hydration of mortars tends to decrease for increasing dosages of accelerator AK (Fig. 5.c).

In mortar AK_10%, a shoulder related to the early formation of AFm phases due to the accelerated C_3A hydration is observed around 1.5 h (Fig. 4.c). In a lower extent, this process may also be observed during the induction period in mortar AK_5.0% (Fig. 4.c). The early formation of AFm phases fills up the space in the matrix before the onset of alite hydration and the precipitation of these phases on the surface of cement particles reduces their solubility and further hydration. Hence, the mortar produced with AK_10% presents lower reaction rates and lower values of heat flow if compared to mortars produced with lower dosages of this accelerator (Table 4).

3.2. Needle penetration test

Fig. 6 presents the average results of needle penetration resistance in sprayed mortars. In each figure, the penetration resistance values of 3.5 and 27.6 MPa are indicated, corresponding to the initial and final setting times presented in ASTM C-403 [4]. Points marked with an 'X' in each curve represent the inflection points of the penetration resistance evolution. Table 5 shows relevant parameters extracted from the Fig. 6.

The initial penetration resistance depends on accelerator type and dosage, as expected. The development of mechanical strength

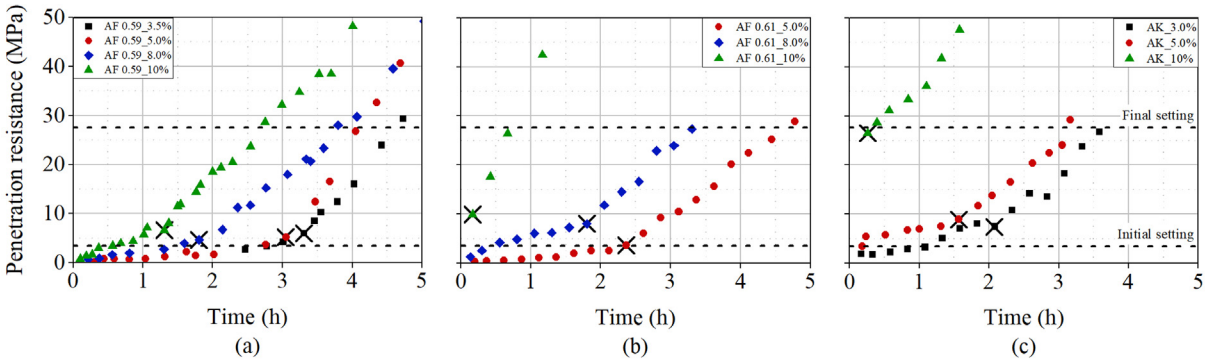

Fig. 6. Average values of needle penetration resistance obtained in sprayed mortars containing accelerator AF 0.59 (a), AF 0.61 (b) and AK (c). Points marked with an 'X' in each curve represent the inflection points of the penetration resistance evolution.

Table 5
Parameters related to the penetration resistance curves.

Mortar	Initial setting time (h)	Final setting time (h)	Slope before inflection point (MPa/h)	Slope after inflection point (MPa/h)
AF 0.59_3.5%	2.8	4.6	1.4	15.1
AF 0.59_5.0%	2.6	4.1	1.5	18.0
AF 0.59_8.0%	1.5	3.8	2.5	12.5
AF 0.59_10%	0.6	2.7	5.8	12.1
AF 0.61_5.0%	2.4	4.6	1.3	10.6
AF 0.61_8.0%	0.4	3.3	5.0	12.8
AF 0.61_10%	–	0.7	Not applicable	32.9*
AK_3.0%	1.1	3.6	3.9	12.6
AK_5.0%	0.2	3.2	6.6	13.9
AK_10%	–	0.3	Not applicable	14.9*

* The first point detected in the curve was used as the initial value to determine the slope.

in sprayed mortars immediately after spraying is directly related to the formation and growth of ettringite and AFm nanocrystals due to accelerator reaction [34,36]. Since the amount of aluminate hydrates precipitated is proportional to the aluminum content in the accelerator formulation (Table 2), the higher the accelerator dosage, the faster the mechanical strength develops after spraying.

The inflection point occurs for penetration resistance values above 3.5 MPa, that is, after the initial setting time of the mortar (see Fig. 6). This indicates that the initial setting time depends strongly on accelerator reactivity. Sprayed mortars present shorter initial setting times and higher rates of strength evolution (steeper slope before the inflection point) for increasing dosages of accelerators (Table 5). Therefore, these chemicals clearly work as set accelerators.

After the inflection point, the evolution of penetration resistance depends on cement hydration. The rate of penetration resistance evolution (slope after inflection point given in Table 5) is directly related to the rate of cement hydration (slope acceleration - main peak, Table 4). Therefore, the higher the rate of cement hydration, the higher the rate of penetration resistance development.

In mortars produced with accelerator AF 0.59, the penetration resistance after the inflection point is the highest when accelerator dosage is equal to 5.0% bcw. Above that dosage, the amount of ettringite formed by accelerator reaction increases and may suppress alite hydration due to lack of space. Therefore, the rate of penetration resistance development reduces because the rate of C-S-H formation decreases.

When accelerators AF 0.61 and AK are employed in the intermediate dosage, the rate of cement hydration (Table 4) and penetration evolution (Table 5) are the highest. Although the hydration rate decreases when the highest accelerator dosage is employed (Table 4), the rate of penetration resistance development increases. This occurs because mortars AF 0.61_10% and AK_10% behave as under-sulfated, as discussed in the results of isothermal calorimetry (Section 3.1). Therefore, the formation of AFm phases due to accelerated C_3A hydration is the main process responsible for the evolution of penetration resistance after the inflection point. The formation of theses phases before the onset of alite hydration may be detrimental to the development of mechanical strength at late ages [25].

3.3. Pin penetration test

Fig. 7 depicts the average results of indirect compressive strength of sprayed mortars until 24 h. In all mortars, compressive strength values at 4 and 6 h were below the lower detection limit of the equipment (0.8 MPa) and, therefore, are not shown. Mortars produced with accelerator AF 0.61 and AK_3% could not be evaluated due to technical difficulties while performing the tests after spraying. Despite the lack of these data, it is still possible to make relevant considerations regarding this test, due to the full set of available data related to AF 0.59 and the two meaningful evolutions over time recorded for AK mixes.

The development of mechanical strength depends on accelerator type and is closely related to the degree of hydration and the energy released in the main hydration peak in the heat flow curves (Table 4). The rate of strength evolution between 8 and 12 h is higher than the rate in the interval from 12 to 24 h. As observed in isothermal calorimetry, cement hydration is the most significant prior to 12 h, resulting in a faster strength gain. After that time, the rate of strength development reduces due to the deceleration of the hydration process (Fig. 5).

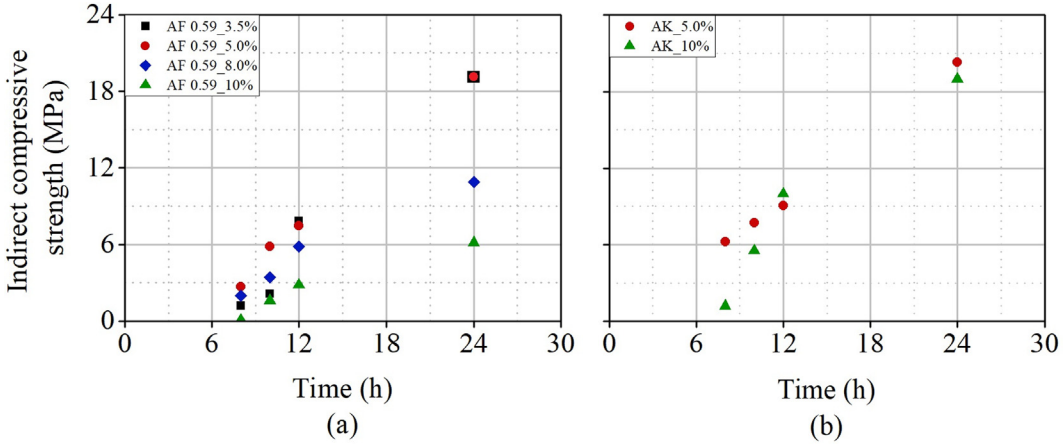

Fig. 7. Average values of indirect compressive strength obtained in sprayed mortars containing accelerator AF 0.59 (a) and AK (b).

The average results of indirect compressive strength tend to be lower for increasing accelerator dosages. As concluded in previous research [25], the determination of indirect compressive strength by the pin penetration test depends mainly of the amount of C-S-H formed during hydration and the values obtained are higher for properly-sulfated systems. Therefore, since alite hydration is suppressed by increasing amounts of aluminate hydrates formed by accelerator reaction, increases in accelerator dosage tend to reduce the compressive strength values from 12 h on, influencing the development of mechanical strengths at late ages negatively. This analysis is corroborated by the determination of the degree of hydration of sprayed mortars (Fig. 5) and it may be inferred that the lower the degree of hydration of the mortar, the lower its indirect compressive strength.

3.4. In situ ultrasound measurements

Fig. 8 depicts a general curve obtained by the continuous monitoring of a sprayed mortar by *in situ* ultrasound measurements. The evolution of ultrasound velocity obtained by the system developed is consistent with findings from prior researches [22,37,38]. The curve contains four different stages, according to the cement hydration process and the consequent development of mechanical strength. Each stage is described subsequently.

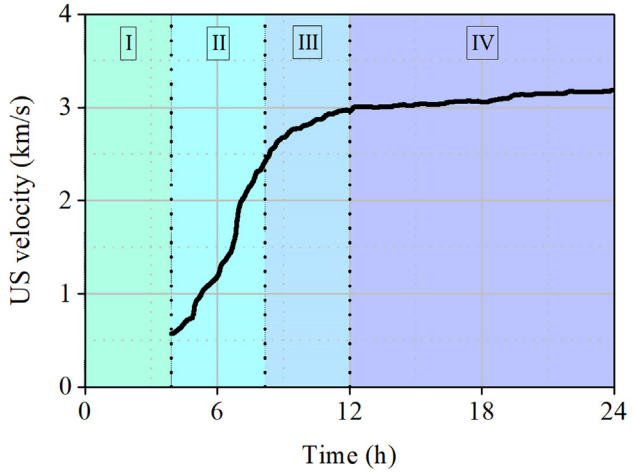

Fig. 8. Designation of 4 stages during the measurement of ultrasound velocity in sprayed mortars.

- **Stage I**: This stage does not present any ultrasound signal. Due to the configuration and geometry of the instrumented panel, with a 20 cm span between transducers, ultrasound velocity must overcome the threshold value of approximately 500 m/s for the signal to be detected. To reach that value, the matrix needs to present proper solid phase interconnectivity, which depends on accelerator reaction and cement hydration processes.
- **Stage II**: Ultrasound signals start to be recorded and ultrasound velocity increases over time. This occurs due to the progress of cement hydration and microstructure development, which improves the interconnectivity of solid particles, increases the solid/liquid ratio of the matrix and reduces porosity. The faster the hydration reactions, the faster the rate of the increase in ultrasound propagation velocity (Fig. 4).
- **Stage III**: The rate of increase of ultrasound velocity starts to descend. This occurs because the matrix presents a significant hardening and cement hydration rates reduce significantly, leading to a reduction in the rate of ultrasound velocity increase.
- **Stage IV**: ultrasound velocity tends to stabilize, because the hydration rate decelerates significantly and the matrix has a porous structure that limits ultrasound velocity [39,40].

Fig. 9 presents the ultrasound velocity curves in sprayed mortars and Table 6 shows relevant parameters extracted from each curve according to each stage observed. Firstly, it is possible to observe that the system developed could monitor continuously the evolution of early age properties of sprayed mortars, as expected. By using the instrumented panel, no decoupling was observed, representing a significant advance in the characterization of sprayed materials [23]. This has already been observed in the characterization of conventional concrete [30], but no references were found regarding the continuous monitoring of sprayed materials. Therefore, this achievement may result in a potential system to characterize sprayed materials continuously in field applications.

Clear changes in the behavior of mortars were observed when different accelerators and dosages were employed. In mortars produced with the lowest dosage of each accelerator, the time required to overcome the ultrasound velocity threshold value of 500 m/s was the longest. As accelerator dosage increases, the duration of stage I reduces.

This occurs because the solid phase interconnectivity and the solid/liquid ratio of the matrix, which are key parameters to provide ultrasound propagation, depend on the amount of aluminate

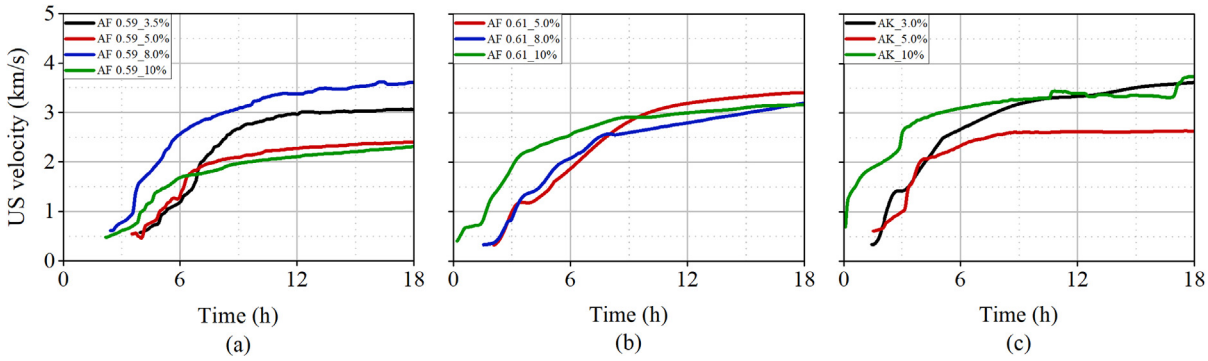

Fig. 9. Evolution of ultrasound propagation velocity obtained in sprayed mortars containing accelerator AF 0.59 (a), AF 0.61 (b) and AK (c).

Table 6
Parameters extracted from the ultrasound velocity curves.

Mortar	Time to overcome threshold value (duration of stage I) (h)	Slope stage II (m/s.h)	Slope stage III (m/s.h)	Duration of stage II + III (h)	Beginning of stage IV (h)
AF 0.59_3.5%	3.9	473	122	8.2	12.1
AF 0.59_5.0%	3.5	462	77	8.0	11.5
AF 0.59_8.0%	2.4	538	143	8.4	10.8
AF 0.59_10%	2.1	367	105	7.4	9.5
AF 0.61_5.0%	2.0	750	300	9.2	11.2
AF 0.61_8.0%	1.6	780	298	8.2	9.8
AF 0.61_10%	0.2	561	148	8.2	8.4
AK_3.0%	1.6	809	157	8.8	10.4
AK_5.0%	1.5	976	149	6.4	7.9
AK_10%	0.1	509	112	7.1	7.2

hydrates formed by accelerator reaction. In addition, the time required to overcome the threshold value depends on the rate of cement hydration, because the phases formed fill up the pores of the matrix. A linear correlation between the time the inflection point occurs in the penetration resistance analysis (Fig. 6) and the time required to overcome the threshold value in ultrasound measurements (Table 6) may be observed in Fig. 10.

Mortars produced with accelerator AK present shorter stage I durations than mortars containing alkali-free accelerators. The early formation of AFm phases by accelerator reaction and C_3A hydration is responsible for that fact [41] because the elastic modulus of these phases is around 2 times higher than the elastic modulus of ettringite and C-S-H (E_{AFm} = 42.3 GPa [41]; $E_{Ettringite}$ = 22.4 GPa [41]; $E_{C\text{-}S\text{-}H}$ = 21.7 GPa [39]). Therefore, under-sulfated systems may overcome the threshold value of ultrasound velocity faster than properly-sulfated systems.

During stage II, the rate of increase in ultrasound velocity is controlled by the precipitation of C-S-H and aluminate hydrates due to alite and C_3A hydration, respectively. Mortars containing high dosages of accelerator present the lowest rates of ultrasound velocity increase. This occurs because the large amount of aluminate phases formed by accelerator reaction suppresses alite hydration and the consequent pore filling caused by the formation of C-S-H. Although the correlation obtained in Fig. 11 is poor when compared to Fig. 10, it may be observed that the slope from stage II in ultrasound measurements is somewhat similar to the slope from the acceleration period in the heat flow curves.

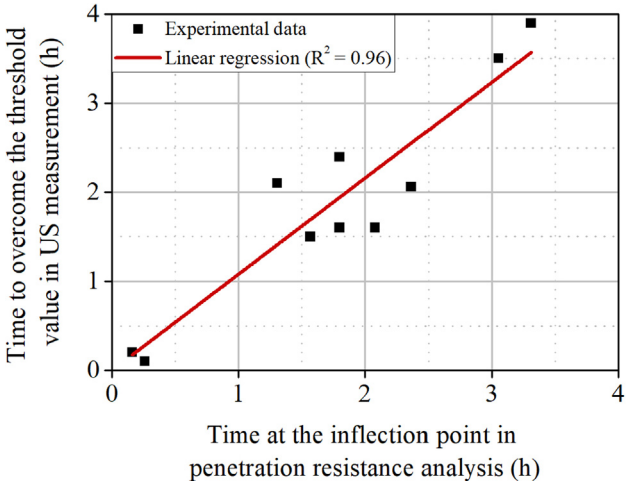

Fig. 10. Relationship between the time the inflection point occurs in the penetration resistance analysis and the time required to overcome the threshold value in ultrasound measurements.

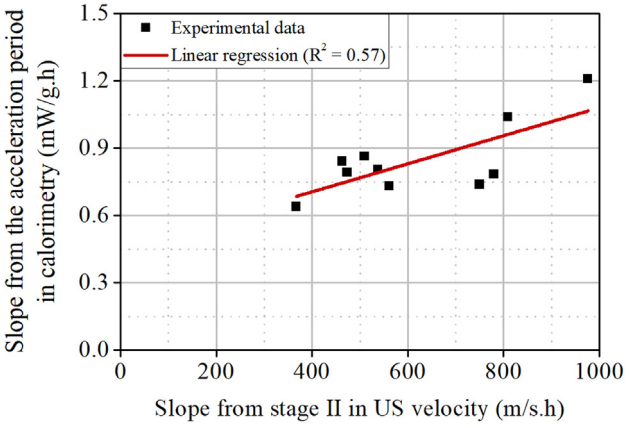

Fig. 11. - Relationship between the slope from stage II in ultrasound measurements and slope from the acceleration period in the heat flow curves.

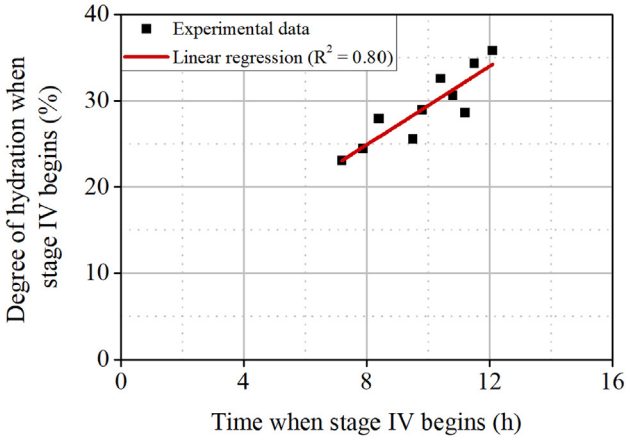

Fig. 12. Relationship between the beginning of stage IV in ultrasound measurements and the degree of hydration of sprayed mortars when stage IV begins.

In addition, the formation of aluminate hydrates by accelerator reaction leads to a fast stiffening of the mortar. Consequently, mortars sprayed with accelerators lose their plasticity immediately after spraying, limiting handling operations. Since sprayed mixes do not undergo consolidation such as conventional mixes, the air entrapped due to spraying is not eliminated [25]. Therefore, mortars are more porous when high dosages of accelerator are employed, reducing the rate of ultrasound velocity increase in stage II.

Stage III represents the final part of the acceleration period in the heat flow curves determined in isothermal calorimetry (Fig. 4). The slope of the ultrasound velocity vs time curve during stage III is lower than the slope from stage II. This means that ultrasound velocity increases at a lower rate in stage III due to the deceleration of hydration reactions [22,23]. The duration of stage II summed with the duration of stage III (Table 6) corresponds to the time required to reach the maximum heat flow in the curves obtained by isothermal calorimetry (Table 4).

The time when stage IV begins corresponds to the time deceleration period starts. As cement hydration rates decreases significantly due to the hardening of the matrix, ultrasound velocity tends to stabilize. As may be observed in Fig. 12, the time when stage IV begins may be related to the degree of hydration of the mortars.

4. Considerations on the determination of initial and final setting times

The initial setting time of a cementitious matrix is defined as the time this matrix begins to lose its plasticity [42]. When mortars and concretes are sprayed with accelerators, their plasticity is lost immediately after spraying, limiting handling operations. Therefore, using the penetration resistance value of 3.5 MPa to determine the initial setting time may not be feasible for sprayed materials.

In addition, initial setting times determined according to ASTM C-403 [4] fell within the stage I period in ultrasound measurements, before the threshold value of ultrasound velocity (500 m/s) was overcome. Therefore, initial setting times could not be correlated to ultrasound velocity. This limitation occurred due to the configuration and geometry of the instrumented panel. To reduce the threshold value and optimize the data acquisition of the equipment, authors suggest the reduction of the distance between transducers (from 20 cm to 10 cm) and the installation of transducers with higher frequency (200 kHz).

The final setting time of a cementitious matrix refers to the time this matrix loses its plasticity and begins to develop mechanical strength [42]. Ultrasound measurements may be successfully used to determine the final setting time of conventional cementitious matrices. Former studies concluded that the final setting time occurs when ultrasound velocity reaches 1.5 km/s [38]. This value may also be adopted to evaluate the final setting time of mortars containing accelerators [23].

However, in the experiments performed in this research, no direct correlation was obtained between final setting times and ultrasound velocity. All the correlations tested showed R^2 values below 0.20 and, therefore, are not presented here. A more representative approach would be to define the final setting time of sprayed materials as the time the inflection point occurs in penetration resistance results (Fig. 6). From that point on, the development of mechanical strength of the matrix increases at a constant rate. Besides, ultrasound measurements are registered because the threshold value has been surpassed, as observed in Fig. 9 and Table 6.

5. Conclusions

The following conclusions may be drawn according to the results obtained in this study:

- The instrumented panel developed may be considered a reliable tool to monitor the evolution of early age properties of sprayed mortars continuously. This method may result in a potential system to characterize sprayed materials continuously in field applications. Nevertheless, the configuration of the test may be further investigated, to reduce the variation of absolute ultrasound velocity and the threshold value. Reducing the distance between transducers and using 200 kHz transducers are recommended.
- By using the system developed, significant changes were observed in the behavior of sprayed mortars depending on the type and dosage of the accelerator employed. The higher the dosage of the accelerator, the faster the threshold value of the ultrasound velocity is reached. Therefore, the system developed may be feasible to characterize the reactivity between cement and accelerator.
- Four different hydration stages could be delimited in ultrasound velocity curves. Each stage corresponds to a hydration period observed in the heat flow curves obtained by isothermal calorimetry. Stage I corresponds to the time required for the onset of the acceleration period, stage II to the acceleration period, stage III to the final part of the acceleration period until the maximum heat flow is reached and stage IV to the deceleration period.
- A correlation was found between the time the threshold value of the ultrasound velocity was reached and the inflection point in the evolution of penetration resistance test. Before the inflection point, no ultrasound signal could be recorded. After the inflection point, ultrasound signals were obtained, because cement hydration rate increases significantly, forming C-S-H, which improves the interconnectivity among solid particles.

CRediT authorship contribution statement

F. Pellegrino: Conceptualization, Formal analysis, Investigation, Methodology, Writing - original draft. **R. Salvador:** Formal analysis, Writing - original draft, Writing - review & editing. **I. Segura:** Conceptualization, Methodology, Supervision, Funding acquisition, Project administration. **S. Aparicio:** Data curation, Investigation, Software. **M.G. Hernández:** Conceptualization, Investigation,

Writing - review & editing. **J.J. Anaya:** Conceptualization, Investigation, Methodology, Software. **S.H. Cavalaro:** Conceptualization, Investigation, Writing - review & editing.

Declaration of Competing Interest

The authors declare that they have no known competing financial interests or personal relationships that could have appeared to influence the work reported in this paper.

Acknowledgements

This research was financially supported by the project RTC-2015- 3185-4 (MAPMIT), co-funded by the Ministerio de Economía y Competitividad of Spain in the Call Retos-Colaboración 2015 and by the European Union through FEDER funds under the objective of promoting the technological development, innovation and high quality research. Furthermore, the authors thank Industrias Quimicas del Ebro (IQE) and, especially, Dr. Miguel Cano and Dr. Jorge Pérez for their active collaboration and technical support on accelerating admixtures. Finally, authors extend their acknowledgements to the staff at the Laboratory of Technology of Structures Luis Agulló and, especially, Robert and Jordi for their technical support on the experimental campaign.

References

[1] E. Villaescusa, Geotechnical Design for Sublevel Open Stoping, 1st ed., CRC Press, 2014.
[2] I. Galan, A. Baldermann, W. Kusterle, M. Dietzel, F. Mittermayr, Durability of shotcrete for underground support– Review and update, Constr. Build. Mater. 202 (2019) 465–493, https://doi.org/10.1016/j.conbuildmat.2018.12.151.
[3] H.A. Saw, E. Villaescusa, C.R. Windsor, A.G. Thompson, Surface support capabilities of freshly sprayed fibre reinforced concrete and safe re-entry time for underground excavations, Tunn. Undergr. Sp. Technol. 64 (2017) 34–42, https://doi.org/10.1016/j.tust.2017.01.005.
[4] American Society for Testing Materials, ASTM C 403 Standard test method for time of setting of concrete mixtures by penetration resistance, West Conshohocken, 2008. doi:10.1520/E0336-11.the.
[5] R.P. Salvador, D.A.S. Rambo, R.M. Bueno, K.T. Silva, A.D. de Figueiredo, On the use of blast-furnace slag in sprayed concrete applications, Constr. Build. Mater. 218 (2019) 543–555, https://doi.org/10.1016/j.conbuildmat.2019.05.132.
[6] I. Galobardes, S.H.P. Cavalaro, C.I. Goodier, S. Austin, Á. Rueda, Maturity method to predict the evolution of the properties of sprayed concrete, Constr. Build. Mater. 79 (2015) 357–369, https://doi.org/10.1016/j.conbuildmat.2014.12.038.
[7] Spanish Association for Standardization, UNE-EN 14488-2, Testing sprayed concrete. Part 2: Compressive strength of young sprayed concrete., (2007).
[8] I. Galobardes, Characterization and control of wet-mix sprayed concrete with accelerators PhD Thesis, Polytechnic University of Catalonia, 2013.
[9] G. Trtnik, M. Gams, Recent advances of ultrasonic testing of cement-based materials at early ages, Ultrasonics. 54 (1) (2014) 66–75, https://doi.org/10.1016/j.ultras.2013.07.010.
[10] H.W. Reinhardt, A.T. Herb, Ultrasonic monitoring of setting and hardening of cement mortar- A new device, 33 (2000) 3–5.
[11] T. Voigt, C.U. Grosse, Z. Sun, S.P. Shah, H.W. Reinhardt, Comparison of ultrasonic wave transmission and reflection measurements with P- and S-waves on early age mortar and concrete, Mater. Struct. 38 (2005) 729–738, https://doi.org/10.1617/14267.
[12] D. Lootens, M. Schumacher, M. Liard, S.Z. Jones, D.P. Bentz, S. Ricci, V. Meacci, Continuous strength measurements of cement pastes and concretes by the ultrasonic wave reflection method, Constr. Build. Mater. 242 (2020) 117902, https://doi.org/10.1016/j.conbuildmat.2019.117902.
[13] C. Herrera-Mesen, R.P. Salvador, S.H.P. Cavalaro, A. Aguado, Effect of gypsum content in sprayed cementitious matrices: Early age hydration and mechanical properties, Cem. Concr. Compos. 95 (2019) 81–91, https://doi.org/10.1016/j.cemconcomp.2018.10.015.
[14] G. Trtnik, G. Turk, F. Kavčič, V.B. Bosiljkov, Possibilities of using the ultrasonic wave transmission method to estimate initial setting time of cement paste, Cem. Concr. Res. 38 (11) (2008) 1336–1342, https://doi.org/10.1016/j.cemconres.2008.08.003.
[15] N. Robeyst, C.U. Grosse, N. De Belie, Measuring the change in ultrasonic p-wave energy transmitted in fresh mortar with additives to monitor the setting, Cem. Concr. Res. 39 (10) (2009) 868–875, https://doi.org/10.1016/j.cemconres.2009.06.016.
[16] B. Desmet, K.C. Atitung, M.A. Abril Sanchez, J. Vantomme, D. Feys, N. Robeyst, K. Audenaert, G. De Schutter, V. Boel, G. Heirman, Ö. Cizer, L. Vandewalle, D. Van Gemert, D. Van Gemert, Monitoring the early-age hydration of self-compacting concrete using ultrasonic p-wave transmission and isothermal calorimetry, Mater. Struct. 44 (8) (2011) 1537–1558, https://doi.org/10.1617/s11527-011-9717-x.
[17] N. Robeyst, E. Gruyaert, C.U. Grosse, N. De Belie, Monitoring the setting of concrete containing blast-furnace slag by measuring the ultrasonic p-wave velocity, Cem. Concr. Compos. 38 (10) (2008) 1169–1176, https://doi.org/10.1016/j.cemconres.2008.04.006.
[18] C.W. Chung, P. Suraneni, J.S. Popovics, L.J. Struble, Using ultrasonic wave reflection to monitor false set of cement paste, Cem. Concr. Compos. 84 (2017) 10–18, https://doi.org/10.1016/j.cemconcomp.2017.08.010.
[19] T. Voigt, Z. Sun, S.P. Shah, Comparison of ultrasonic wave reflection method and maturity method in evaluating early-age compressive strength of mortar, Cem. Concr. Compos. 28 (4) (2006) 307–316, https://doi.org/10.1016/j.cemconcomp.2006.02.003.
[20] M. Molero, I. Segura, S. Aparicio, M.G. Hernández, M.A.G. Izquierdo, On the measurement of frequency-dependent ultrasonic attenuation in strongly heterogeneous materials, Ultrasonics. 50 (8) (2010) 824–828, https://doi.org/10.1016/j.ultras.2010.04.006.
[21] D. AGGELIS, D. POLYZOS, T. PHILIPPIDIS, Wave dispersion and attenuation in fresh mortar: Theoretical predictions vs. experimental results, J. Mech. Phys. Solids. 53 (4) (2005) 857–883, https://doi.org/10.1016/j.jmps.2004.11.005.
[22] N. De Belie, C.U. Grosse, J. Kurz, H.-W. Reinhardt, Ultrasound monitoring of the influence of different accelerating admixtures and cement types for shotcrete on setting and hardening behaviour, Cem. Concr, Res. 35 (11) (2005) 2087–2094, https://doi.org/10.1016/j.cemconres.2005.03.011.
[23] R.P. Salvador, S.H.P. Cavalaro, I. Segura, M.G. Hernández, J. Ranz, A.D.d. Figueiredo, Relation between ultrasound measurements and phase evolution in accelerated cementitious matrices, Mater. Des. 113 (2017) 341–352, https://doi.org/10.1016/j.matdes.2016.10.022.
[24] H.F.W. Taylor, Cement chemistry, 2nd ed., Thomas Telford Publishing, London, 1997.
[25] R.P. Salvador, S.H.P. Cavalaro, R. Monte, A.D. Figueiredo, Relation between chemical processes and mechanical properties of sprayed cementitious matrices containing accelerators, Cem. Concr. Compos. 79 (2017) 117–132, https://doi.org/10.1016/j.cemconcomp.2017.02.002.
[26] Spanish Association for Standardization, UNE-EN 14488-1:2006, Testing Sprayed Concrete - Part 1: Sampling Fresh and Hardened Concrete, (2006).
[27] R.P. Salvador, S.H.P. Cavalaro, I. Segura, A.D. Figueiredo, J. Pérez, Early age hydration of cement pastes with alkaline and alkali-free accelerators for sprayed concrete, Constr. Build. Mater. 111 (2016) 386–398, https://doi.org/10.1016/j.conbuildmat.2016.02.101.
[28] S. Aparicio Secanellas, M.G. Hernández, I. Segura, M. Morata, J.J. Anaya, A system designed to monitor in-situ the curing process of sprayed concrete, Constr. Build. Mater. 224 (2019) 823–834, https://doi.org/10.1016/j.conbuildmat.2019.07.117.
[29] Windsor pin system WP-2000. Instruction manual, (2010) 25.
[30] J. Ranz, S. Aparicio, J.V. Fuente, J.J. Anaya, M.G. Hernández, Monitoring of the curing process in precast concrete slabs: An experimental study, Constr. Build. Mater. 122 (2016) 406–416, https://doi.org/10.1016/j.conbuildmat.2016.06.041.
[31] S. Aparicio, J. Ranz, R. Galán, E. Villanueva, M.G. Hernández, J.J. Anaya, M.A.G. Izquierdo, J.V. Fuente, R. Fernández, V. Ciscar, V. Albert, Procedimiento y sistema inalámbrico de medida del grado de fraguado y endurecimiento de materiales cementicios para la predicción de resistencias mecánicas. PCT/ES2012/070439, 2012.
[32] R.P. Salvador, S.H.P. Cavalaro, M. Cincotto, A.D. Figueiredo, Parameters controlling early age hydration of cement pastes containing accelerators for sprayed concrete, Cem. Concr. Res. J. 89 (2016) 230–248. doi:10.1016.
[33] L.G. Briendl, F. Mittermayr, A. Baldermann, F.R. Steindl, M. Sakoparnig, I. Letofsky-Papst, I. Galan, Early hydration of cementitious systems accelerated by aluminium sulphate: Effect of fine limestone, Cem. Concr. Res. 134 (2020) 106069, https://doi.org/10.1016/j.cemconres.2020.106069.
[34] R.P. Salvador, S.H.P. Cavalaro, M. Cano, A.D. Figueiredo, Influence of spraying on the early hydration of accelerated cement pastes, Cem. Concr. Res. 88 (2016) 7–19, https://doi.org/10.1016/j.cemconres.2016.06.005.
[35] P. Juilland, Early Hydration of Cementitious Systems. PhD Thesis, Federal Polytechnic School of Lausanne, 2009.
[36] C. Maltese, C. Pistolesi, A. Bravo, T. Cerulli, D. Salvioni, M. Squinzi, Formation of nanocrystals of AFt phase during the reaction between alkali-free accelerators and hydrating cement: a key factor for sprayed concretes setting and hardening, RILEM Proc, F. Full J. TitleRILEM Proc. PRO 45 (2005) 329–338.

[37] J. Carette, S. Staquet, Monitoring the setting process of mortars by ultrasonic P and S-wave transmission velocity measurement, Constr. Build. Mater. 94 (2015) 196–208, https://doi.org/10.1016/j.conbuildmat.2015.06.054.
[38] H.W. Reinhardt, C.U. Grosse, Continuous monitoring of setting and hardening of mortar and concrete, Constr. Build. Mater. 18 (3) (2004) 145–154, https://doi.org/10.1016/j.conbuildmat.2003.10.002.
[39] G. Constantinides, F.-J. Ulm, The effect of two types of C-S-H on the elasticity of cement-based materials: Results from nanoindentation and micromechanical modeling, Cem. Concr. Res. 34 (1) (2004) 67–80, https://doi.org/10.1016/S0008-8846(03)00230-8.
[40] M.G. Hernández, J.J. Anaya, L.G. Ullate, M. Cegarra, T. Sanchez, Application of a micromechanical model of three phases to estimating the porosity of mortar by ultrasound, Cem. Concr. Res. 36 (4) (2006) 617–624, https://doi.org/10.1016/j.cemconres.2004.07.018.
[41] S. Kamali, M. Moranville, E. Garboczi, S. Prené, B. Gerard, Hydrate dissolution influence on the Young' s modulus of cement pastes, in: Proc. 5th Int. Conf. Fract. Mech. Concr. Concr. Struct. Vail, USA, 2004: pp. 631–638.
[42] P.D.P. Kumar Mehta, P.D. Paulo, J.M. Monteiro, Concrete: Microstructure, Properties, and Materials, 4th ed.,., McGraw-Hill Education, New York, 2014.